

# Nonlinear spectroscopy of rubidium: an undergraduate experiment

V Jacques, B Hingant, A Allafort, M Pigeard  
and J F Roch

Département de Physique, Ecole Normale Supérieure de Cachan, 61 avenue du Président Wilson,  
94235 Cachan, France

E-mail: [vincent.jacques@lpqm.ens-cachan.fr](mailto:vincent.jacques@lpqm.ens-cachan.fr)

Received 9 February 2009, in final form 14 April 2009

Published 8 July 2009

Online at [stacks.iop.org/EJP/30/921](http://stacks.iop.org/EJP/30/921)

## Abstract

In this paper, we describe two complementary nonlinear spectroscopy methods which both allow one to achieve Doppler-free spectra of atomic gases. First, saturated absorption spectroscopy is used to investigate the structure of the  $5S_{1/2} \rightarrow 5P_{3/2}$  transition in rubidium. Using a slightly modified experimental setup, Doppler-free two-photon absorption spectroscopy is then performed on the  $5S_{1/2} \rightarrow 5D_{5/2}$  transition in rubidium, leading to accurate measurements of the hyperfine structure of the  $5D_{5/2}$  energy level. In addition, electric dipole selection rules of the two-photon transition are investigated, first by modifying the polarization of the excitation laser, and then by measuring two-photon absorption spectra when a magnetic field is applied close to the rubidium vapour. All experiments are performed with the same grating-feedback laser diode, providing an opportunity to compare different high-resolution spectroscopy methods using a single experimental setup. Such experiments may acquaint students with quantum mechanics selection rules, atomic spectra and Zeeman effect.

(Some figures in this article are in colour only in the electronic version)

## 1. Introduction

The development of laser diode devices about 30 years ago is nowadays regarded as an indisputable breakthrough either for the growth of a broad range of technological applications or for its huge impact on atom physics research, from high-resolution spectroscopy to laser-cooling techniques. Although the spectral properties and the tunability of these lasers may prove unsuited for some applications, an efficient device can be built by stabilizing the diode using an optical feedback from an external grating operating in Littrow configuration [1, 2]. One can thus easily obtain a low-cost narrow band laser with several tens of milliWatts of optical power and a mode-hop-free frequency tuning which can be larger than 50 GHz.

Such tunable laser diodes are useful tools for teaching atom physics in advanced undergraduate laboratory courses. Indeed, many experiments have been developed for undergraduates using these devices in the past years, ranging from atomic hyperfine structure studies of rubidium and cesium [3, 4], to interferometric measurements of the resonant absorption and refractive index in rubidium gas [5], temperature dependence of Doppler-broadening [6], observation of Faraday effect [7] and two-photon spectroscopy in rubidium [8].

In this paper, we use a simple grating-feedback laser diode to investigate the hyperfine structure of the  $5P_{3/2}$  and  $5D_{5/2}$  excited states in rubidium. This is achieved following two different methods of Doppler-free high-resolution spectroscopy. First, saturated absorption spectroscopy is performed on the  $5S_{1/2} \rightarrow 5P_{3/2}$  transition in rubidium to measure the hyperfine structure of the  $5P_{3/2}$  excited state. Using the same laser diode and a slightly modified experimental setup, Doppler-free two-photon absorption spectroscopy is then performed on the transition  $5S_{1/2} \rightarrow 5D_{5/2}$ , leading to accurate measurements of the hyperfine structure of the  $5D_{5/2}$  energy level. These two techniques, both based on nonlinear interaction of light with atoms, are complementary since they enable us to probe atomic transitions following different electric dipole selection rules. Indeed, for single-photon transitions involved in saturated absorption spectroscopy, the orbital angular momentum  $l$  must satisfy the selection rule  $\Delta l = \pm 1$ . Consequently, transitions have to involve ground and excited states with opposite parity. Contrarily, selection rules for two-photon transitions become  $\Delta l = 0, \pm 2$ , allowing one to investigate transitions between levels of identical parity.

In the following, we begin by providing a general description of the experimental apparatus used to perform the experiments. We then briefly discuss Doppler broadening and describe Doppler-free saturation absorption spectroscopy of the  $5S_{1/2} \rightarrow 5P_{3/2}$  transition in rubidium, which is the simplest undergraduate experiment using a tunable laser diode [3, 4]. Afterwards, the hyperfine structure of the excited state  $5D_{5/2}$  is probed using Doppler-free two-photon absorption spectroscopy. In addition, electric dipole selection rules of the two-photon transition are investigated, first by modifying the polarization of the excitation laser, and then by measuring two-photon absorption spectra when the rubidium vapour cell is placed in a magnetic field. Such experiments provide an opportunity to compare different high-resolution spectroscopy methods using a single experimental setup and may acquaint students with quantum mechanics selection rules, atomic spectra and Zeeman effect.

## 2. Experimental apparatus

All experiments are performed with a commercial grating-feedback laser diode (Toptica Photonics, DL100) operating in Littrow configuration [9]. Such a laser diode, stabilized in temperature, has a typical free-running wavelength of 780 nm with 1 MHz linewidth and an output power of 30 mW. Besides, a 30 dB optical isolator (Electro-Optics Technologies) is used to prevent laser instability caused by optical feedback in the laser diode cavity.

Preliminary tuning of the laser diode emission wavelength close to a resonant transition of rubidium is achieved by manually changing the length of the external cavity and by monitoring the output wavelength using a commercial wavelength-meter [10]. Scanning the frequency of the laser diode is then realized by applying a voltage ramp to a piezoelectric transducer which changes the external cavity length and thus the emission wavelength. With Toptica DL100 commercial diode, a mode-hop free frequency tuning around 20 GHz is easily achieved.

Part of the laser emission is constantly sent into a homemade Fabry–Perot interferometer (FPI), with a 750 MHz free-spectral-range and a finesse  $\mathcal{F} = 10$ , whose transmission peaks provide a frequency reference for the measurements of rubidium spectral features. A rubidium

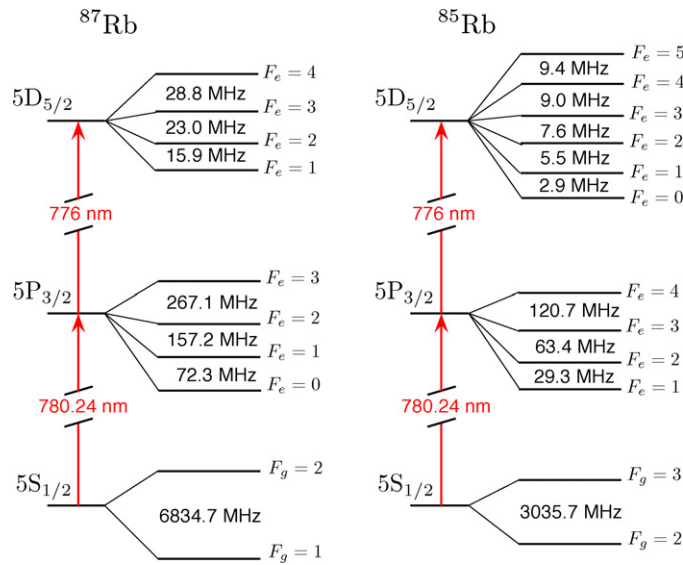


Figure 1. Energy-level diagram for  $^{85}\text{Rb}$  and  $^{87}\text{Rb}$ .

vapour cell containing  $^{85}\text{Rb}$  (72% natural abundance) and  $^{87}\text{Rb}$  (28% natural abundance) from Thorlabs is used. The energy-level diagram of the relevant transitions in rubidium is shown in figure 1.

### 3. Doppler broadening of absorption spectra

In conventional laser spectroscopy, atomic hyperfine structure is often hidden by inhomogeneous Doppler broadening. Indeed, when atoms in a vapour cell are irradiated by a laser beam at frequency  $\nu_L$  in the laboratory frame of reference, they experience in their own frame a Doppler shifted laser frequency  $\nu$ , related to the atom velocity  $v_z$  along the incident light direction  $z$  as

$$\nu = \nu_L \left[ 1 - \frac{v_z}{c} \right], \quad (1)$$

where  $c$  is the speed of light. This formula is valid in the approximation of non-relativistic atoms  $v_z \ll c$ .

As a result, by scanning the laser frequency  $\nu_L$  around an atomic transition at frequency  $\nu_0$ , the class of atoms with velocity  $v_z$  absorbs light when the condition

$$\nu_L = \frac{\nu_0}{1 - \frac{v_z}{c}} \quad (2)$$

is fulfilled. For atoms in a vapour cell, the probability distribution of velocities  $p(v_z)$  follows a Maxwell–Boltzmann distribution

$$p(v_z) = \sqrt{\frac{m}{2\pi k_b T}} \exp\left(-\frac{mv_z^2}{2k_b T}\right), \quad (3)$$

where  $k_b$  is the Boltzmann constant,  $T$  is the absolute temperature and  $m$  is the mass of the atoms. By substituting equation (2) into equation (3), the relative number of atoms  $N$  which are resonant with the laser at frequency  $\nu_L$ , is given by the Gaussian function

$$N = \exp\left[-\frac{mc^2}{2k_b T} \left(\frac{\nu_0 - \nu_L}{\nu_L}\right)^2\right]. \quad (4)$$

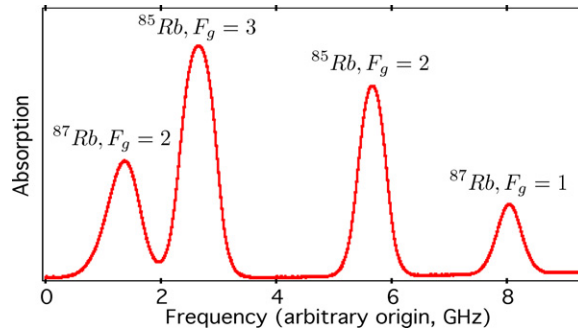


**Figure 2.** Doppler-broadened absorption spectrum related to the transition  $5S_{1/2} \rightarrow 5P_{3/2}$  in rubidium at room temperature. The ground-state hyperfine splitting is measured to be  $3.02 \pm 0.03$  GHz for  $^{85}\text{Rb}$  and  $6.80 \pm 0.07$  GHz for  $^{87}\text{Rb}$ . Excited-state hyperfine structure is hidden by Doppler broadening.

This distribution is directly translated in a Gaussian shape of the atomic medium absorption profile, centred at the resonant frequency  $\nu_0$  and with a full width at half-maximum (FWHM)  $\Delta\nu_{\text{dop}}$  given by

$$\Delta\nu_{\text{dop}} = 2\nu_0 \sqrt{\frac{2k_B T \ln 2}{mc^2}}. \quad (5)$$

For rubidium atoms,  $\Delta\nu_{\text{dop}} \approx 500$  MHz at room temperature, which is smaller than the energy splitting between ground state  $5S_{1/2}$  hyperfine levels but much bigger than that of the excited state  $5P_{3/2}$  (see figure 1).

In order to experimentally observe Doppler broadened absorption spectra, the extended-cavity diode laser is tuned close to the rubidium transition  $5S_{1/2} \rightarrow 5P_{3/2}$  at the wavelength  $\lambda = 780.24$  nm (vacuum wavelength) and directed through the rubidium vapour cell. A typical absorption profile for the  $5S_{1/2} \rightarrow 5P_{3/2}$  transition in rubidium is depicted in figure 2. Ground-state hyperfine levels are resolved whereas the hyperfine structure of the  $5P_{3/2}$  excited state remains hidden by Doppler broadening. Gaussian fit of each absorption line gives a FWHM of  $518 \pm 15$  MHz as expected for Doppler broadening at room temperature [6].

## 4. Doppler-free saturated absorption spectroscopy

### 4.1. Principle

In the early 1970s, Theodor W Hänsch and Christian Bordé independently introduced a method using nonlinear interaction of laser light with atoms to achieve Doppler-free spectra of atomic gases [11–13]. This technique, commonly called saturated absorption spectroscopy, has revolutionized spectroscopy studies [14] and is now widely used in atom physics research as a versatile method to lock laser frequencies on atomic transitions.

In such a technique, two counterpropagating laser beams at identical frequencies  $\nu_L$  interact with atoms in a vapour cell. One beam is denoted  $P$  as a pump beam, and the other one, weaker, is denoted  $S$  and usually called the probe beam. When the laser frequency  $\nu_L$  is different from the frequency  $\nu_0$  of the atomic transition (e.g.  $\nu_L > \nu_0$ ), the pump beam  $P$  interacts with a group of atoms with velocity  $v_z$ , whereas the counterpropagating probe beam  $S$  excites the symmetric group of velocity  $-v_z$ . As a result, the two laser beams interact with

different classes of atom and the absorption spectra are identical to the one obtained using a single laser excitation scheme. However, under the particular circumstance where  $\nu_L = \nu_0$ , both beams interact with the same class of atoms of velocity  $v_z = 0$ . In that case, the pump beam  $P$  saturates the atomic transition, depleting the number of atoms with velocity  $v_z = 0$  in the ground state. As a result, the absorption of the counterpropagating probe beam is decreased, as most of the atoms are already excited by the pump beam. The absorption of the probe beam finally presents a Doppler broadened profile, on which is superimposed a dip corresponding to the resonant frequency  $\nu_0$ , for which both beams are interacting with the same class of atoms  $v_z = 0$ .

Using Bloch equations theory in the approximation of a two-level atom (ground state  $|g\rangle$  and excited state  $|e\rangle$ ), the dip is shown to be Lorentzian with a linewidth  $\Delta\nu$  (FWHM) given by the relation [15]

$$\Delta\nu = 2\sqrt{\gamma^2 + \frac{\Omega_1^2\gamma}{\Gamma_{\text{sp}}}}, \quad (6)$$

where  $2\gamma$  is the natural linewidth of the transition,  $\Gamma_{\text{sp}}$  is the spontaneous emission rate and  $\Omega_1$  is the Rabi frequency associated with the pump beam amplitude  $E_p$  which saturates the atomic transition. The Rabi frequency is given by  $\Omega_1 = -d_{\text{eg}}E_p/\hbar$ , where  $d_{\text{eg}}$  is the value of the dipole operator between states  $|g\rangle$  and  $|e\rangle$ . In principle, Doppler-free saturated absorption spectroscopy should allow one to reach an asymptotic value of the natural linewidth of the transition by decreasing the saturating pump beam intensity  $|E_p|^2$  [16]<sup>1</sup>.

#### 4.2. Crossover resonance

We now consider two atomic transitions at frequencies  $\nu_1$  and  $\nu_2$  ( $\nu_1 < \nu_2$ ) involving a common ground state, with a frequency difference smaller than the Doppler broadening  $\Delta\nu_{\text{dop}}$ .

When the laser frequency is set exactly midway between the two resonances,  $\nu_L = (\nu_1 + \nu_2)/2$ , the pump beam interacts with two classes of atoms of opposite velocities  $v_z$  and  $-v_z$ . Positive velocity atoms  $v_z$  experience the pump beam redshifted to the lower transition frequency  $\nu_1 = \nu_L(1 - v_z/c)$  whereas atoms with negative velocity  $-v_z$  see the pump beam blueshifted to the higher resonance frequency  $\nu_2 = \nu_L(1 + v_z/c)$ . This results in a depletion of the number of atoms with velocities  $\pm v_z$  in the ground state. At the same frequency, the probe beam interacts with exactly the same group of atoms, but in the opposite way as atoms with velocity  $-v_z$  (resp.  $v_z$ ) are resonant with the transition  $\nu_1$  (resp.  $\nu_2$ ). Then, the probe beam absorption profile once again shows a dip, more intense than the one observed for standard resonance as it involves two groups of atom velocities. This dip, usually called a crossover resonance, is peculiar to saturated absorption spectroscopy.

#### 4.3. Experimental setup and results

The experimental setup used to implement Doppler-free saturated absorption spectroscopy of rubidium is described in figure 3(a).

The laser beam, tuned close to the rubidium transition  $5S_{1/2} \rightarrow 5P_{3/2}$ , is first sent through a half-wave plate and a polarizing beam splitter (PBS), used to control the light power entering the rubidium cell. The pump beam  $P$  then travels through the rubidium cell and is retroreflected as a counterpropagating probe beam  $S$  using a mirror and a 1% optical density. A quarter

<sup>1</sup> The lineshape of saturated absorption dips is actually much more complicated than a Lorentzian profile because the method is sensible to velocity-changing collisions. For a precise calculation of the dip profile one can see [16].

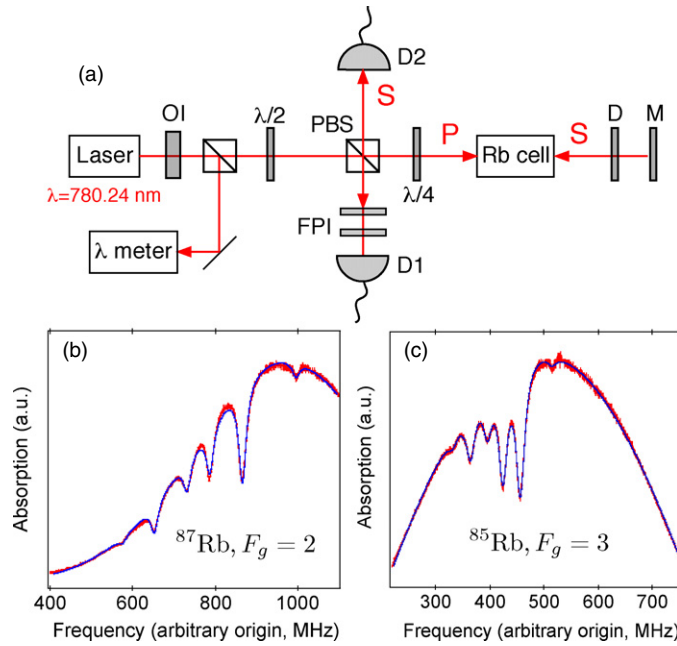


**Figure 3.** Doppler-free saturated absorption spectroscopy of rubidium. (a) Experimental setup. OI, optical isolator;  $\lambda/2$ , half-wave plate;  $\lambda/4$ , quarter-wave plate; PBS, polarization beam splitter; FPI, Fabry-Pérot interferometer; D, optical density (1%); M, mirror; D1 and D2, photodiodes. P and S denote the pump and probe beam, respectively. (b) Saturated absorption spectrum for the transition  $5S_{1/2}, F_g = 2 \rightarrow 5P_{3/2}$  of  $^{87}\text{Rb}$ . Six Doppler-free dips are resolved corresponding from left to right to  $F_g = 2 \rightarrow F_e = 1$ , crossover  $F_e = 1$  and 2,  $F_e = 2$ , crossover  $F_e = 1$  and 3, crossover  $F_e = 2$  and 3, and  $F_e = 3$ . (c) Saturated absorption spectrum for the transition  $5S_{1/2}, F_g = 3 \rightarrow 5P_{3/2}$  of  $^{85}\text{Rb}$ . From left to right the peaks correspond to  $F_e = 2$ , crossover  $F_e = 2$  and 3,  $F_e = 3$ , crossover  $F_e = 2$  and 4, crossover  $F_e = 3$  and 4, and  $F_e = 4$ . Solid lines are data fitting using the product of six Lorentzian functions with a Gaussian profile. For the hyperfine structure of the  $5P_{3/2}$  excited state, we finally obtain  $\delta[(1 \leftrightarrow 2)]_{^{87}\text{Rb}} = 156 \pm 2$  MHz,  $\delta[(2 \leftrightarrow 3)]_{^{87}\text{Rb}} = 264 \pm 3$  MHz,  $\delta[(2 \leftrightarrow 3)]_{^{85}\text{Rb}} = 64 \pm 1$  MHz, and  $\delta[(3 \leftrightarrow 4)]_{^{85}\text{Rb}} = 119 \pm 2$  MHz, where  $\delta[(i \leftrightarrow j)]$  is the energy splitting between hyperfine sublevels  $F_e = i$  and  $F_e = j$ .

wave plate is inserted in order to rotate by  $90^\circ$  the probe beam polarization which is finally reflected by the PBS and detected using a photodiode.

Typical saturated absorption spectra are depicted in figures 3(b) and (c). Within a Gaussian envelope resulting from Doppler broadening, six dips appear, three of them being related to the hyperfine structure of the excited state  $5P_{3/2}$  and the other three corresponding to crossover resonances.

The linewidths of the saturated absorption dips are found equal to  $\Delta\nu = 22 \pm 1$  MHz for  $^{87}\text{Rb}$  and  $\Delta\nu = 20 \pm 1$  MHz for  $^{85}\text{Rb}$ . The lifetime  $\tau$  of the  $5P_{3/2}$  excited state in rubidium is about 28 ns. The natural linewidth predicted by the Heisenberg uncertainty principle is then  $2\gamma = 1/(2\pi\tau) = 6$  MHz, much smaller than the one measured.

As illustrated by equation (6), the spectral linewidth  $\Delta\nu$  of the absorption dips strongly depends on the pump beam intensity which saturates the atomic transition. As such saturation is at the heart of the method, it is hard to reach the natural linewidth using Doppler-free saturated absorption spectroscopy. A possible method would consist in measuring the linewidth of the dips for different pump beam intensities and to take the asymptotic value of the linewidth at

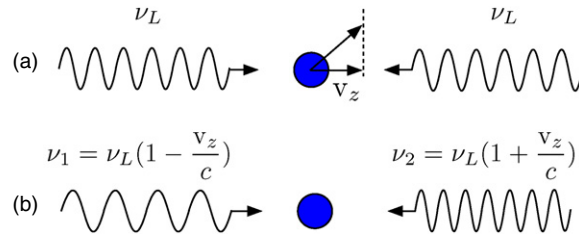


**Figure 4.** Principle of Doppler-free two-photon absorption spectroscopy. (a) An atom interacts with two opposite travelling waves at the same frequency  $\nu_L$  in the laboratory frame of reference. (b) In the atom rest frame, the two frequencies are Doppler shifted to  $\nu_1$  and  $\nu_2$ . By absorbing two photons travelling in opposite directions, the Doppler shifts cancel.

null intensity. However, the obtained value would still be bigger than the natural linewidth because of collisions and inhomogeneous transit time broadening resulting from the finite time of interaction between the atoms and the laser light [16].

In the early 1970s, saturated absorption spectroscopy led to huge improvements in metrology experiments [17]. However, this method is sensible to recoil effect when an atom absorbs or emits a photon, which induces a splitting of the lines [18, 19]. For metrology applications, saturated absorption spectroscopy has thus quickly been superseded by other methods, like Doppler-free two-photon absorption spectroscopy.

## 5. Doppler-free two-photon absorption spectroscopy

The possibility of using two-photon absorption as a Doppler-free spectroscopy method was first proposed by L S Vasilenko, V P Chebotaev and A V Shishaev [20] whereas the first experimental demonstration was simultaneously obtained in 1974 by F Biraben, B Cagnac and G Grynberg [21, 22] in Paris and by M D Levenson and N Bloembergen [23] in Harvard.

Nowadays, Doppler-free two-photon absorption spectroscopy is still the most powerful method for high-precision measurements of fundamental constants like the Lamb shift or the Rydberg constant [24].

### 5.1. Principle

We consider atoms in a vapour interacting with two counterpropagating beams at the same frequency  $\nu_L$  in the laboratory frame of reference (figure 4). In its rest frame, each atom with velocity  $v_z$  interacts with two Doppler-shifted travelling waves at frequencies  $\nu_1$  and  $\nu_2$  which, in the approximation of non-relativistic atoms  $v_z \ll c$ , are equal to

$$\nu_1 = \nu_L \left[1 - \frac{v_z}{c}\right] \quad (7)$$

$$\nu_2 = \nu_L \left[1 + \frac{v_z}{c}\right] \quad (8)$$

We now suppose that the atoms can reach an excited state  $|e\rangle$  (energy  $E_e$ ) by absorbing two photons in the ground state  $|g\rangle$  (energy  $E_g$ ). Using equations (7) and (8), the resonant condition for absorbing two photons travelling in opposite directions is given by

$$E_e - E_g = h\nu_L \left[1 - \frac{v_z}{c}\right] + h\nu_L \left[1 + \frac{v_z}{c}\right] = 2h\nu_L. \quad (9)$$

The terms depending on atom velocity disappear as the two Doppler shift terms cancel. Consequently, when the resonance condition (9) is fulfilled, all the atoms, irrespective of their velocities, can absorb two photons. The line shape of this Doppler-free two-photon absorption resonance is theoretically predicted to be Lorentzian, the width being the natural linewidth  $\gamma$  of the transition [25]. Contrary to saturated absorption spectroscopy, there is no recoil shift using such a method as the total momentum transfer from light to atom is null.

When the resonant condition is not realized, or when the two counterpropagating beams are not well superimposed, the atoms can no longer absorb two photons propagating in opposite directions. However, some atoms can still absorb two photons propagating in the same direction, if their velocity  $v_z$  fulfils the relation  $E_e - E_g = 2h\nu_L [1 \pm \frac{v_z}{c}]$ . Such a process leads to an additional Doppler-broadened profile. However, for a given frequency  $\nu_L$  of the laser, only one class of atom velocities contributes to this Doppler-broadened signal, whereas all the atoms contribute to the resonance signal when the condition (9) is fulfilled. As a result, Doppler-free two-photon absorption spectra appear as the superposition of a Lorentzian curve of large intensity and narrow width, and a Gaussian profile of small intensity and broad width (Doppler width) [25].

Single-photon transitions satisfy the selection rules  $\Delta l = \pm 1$ , where  $l$  is the orbital angular momentum. Such transitions then require ground and excited states of opposite parity, such as the transition  $5S_{1/2} \rightarrow 5P_{3/2}$  investigated using saturated absorption spectroscopy in section 4. For two-photon transitions, the selection rules become  $\Delta l = 0, \pm 2$ , allowing one to investigate transitions between levels of identical parity. In that sense, two-photon spectroscopy is complementary to saturated absorption spectroscopy.

In the following, we investigate the transition  $5S_{1/2} \rightarrow 5D_{5/2}$  of rubidium. Two-photon absorption is achieved by exciting rubidium at the wavelength  $\lambda = 778.1$  nm (vacuum wavelength), and detected by monitoring the fluorescence at 420 nm from the  $5D_{5/2} \rightarrow 6P_{3/2} \rightarrow 5S_{1/2}$  radiative cascade decay (figure 5(a)).

Usually, nonlinear processes such as two-photon transitions require high-power lasers. However, for the case under study, the two-photon transition probability is greatly enhanced because the first excited  $5P_{3/2}$  state is close (2 nm detuning) to the virtual intermediate state involved in the two-photon process (figure 5(a)). Furthermore, the need for high power is also compensated by the fact that all the atoms contribute to the Doppler-free signal whereas saturation spectroscopy only involves a single class of atom with velocity  $v_z = 0$ . Therefore, the experiment can be performed with a simple tunable laser diode [8, 26, 27].<sup>2</sup>

## 5.2. Experimental setup

The experimental setup used to implement Doppler-free two-photon absorption spectroscopy is depicted in figure 5(b).

After preliminary tuning of the laser diode at the wavelength  $\lambda = 778.1$  nm, the laser beam is sent through a half-wave plate and a polarizing beam splitter (PBS). The reflected light on PBS is directed into the Fabry–Perot interferometer for frequency reference while the transmitted part is focused inside the rubidium cell using a pair of collimating lenses. The beam is then retroreflected using a mirror to obtain the required counterpropagating beams configuration. For the present experiment, the laser power entering the rubidium cell is measured equal to 18 mW. A quarter-wave plate is also introduced before the rubidium cell in order to excite the atoms with two counterpropagating beams with identical circular polarizations  $\sigma^+$ . Such a configuration strongly reduces the amount of light reflected into the

<sup>2</sup> The two-photon transition  $5S_{1/2} \rightarrow 5D_{3/2}$  could also be investigated by exciting at the wavelength  $\lambda = 778.2$  nm. In that case the probability of two-photon absorption is however much weaker [28].

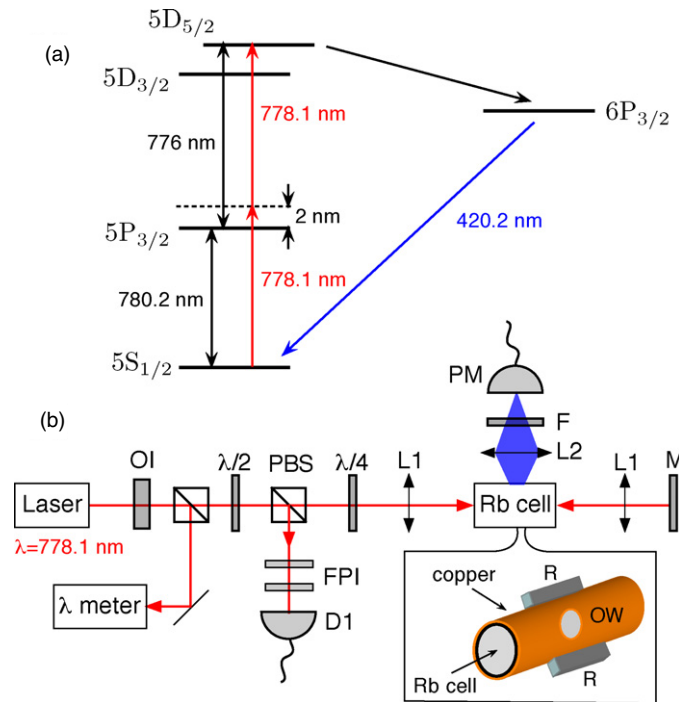


**Figure 5.** (a) Energy levels involved in the two-photon transition  $5S_{1/2} \rightarrow 5D_{5/2}$  of rubidium. (b) Doppler-free two-photon spectroscopy setup. OI, optical isolator;  $\lambda/2$ , half-wave plate; PBS, polarization beamsplitter;  $\lambda/4$ , quarter-wave plate; FPI, Fabry-Perot interferometer; D1, photodiode; L1, 100 mm focal lenses; M, mirror; L2, 60 mm focal lens; F, 10 nm width interference filter centred at 420 nm. PM, photomultiplier. The rubidium cell is inserted in a copper ring, on which a couple of high power resistors (R) are glued in order to heat the cell. An optical window (OW) is cut inside the copper to detect the fluorescence.

laser diode, as the reflected light is mostly cut by the PBS. Even using an optical isolator, we noticed that optical feedback caused instability in the laser output when the quarter-wave plate was removed.

The efficiency of two-photon absorption strongly depends on the atomic vapour temperature [8], which is directly related to the average number of atoms in interaction with the laser in the focal volume. For the studied two-photon transition, it has been shown that the fluorescence signal at 420 nm used to monitor two-photon absorption begins to be efficient for temperature higher than  $80\text{ }^{\circ}\text{C}$  [8]. This signal then increases with temperature until saturation around  $130\text{ }^{\circ}\text{C}$ . At higher temperatures, even if the two-photon absorption probability is still increasing, the fluorescence signal no longer increases because of self-absorption of the  $6P_{3/2} \rightarrow 5S_{1/2}$  transition [26].

Usually the atomic vapour is heated by introducing the cell inside an oven. Here the rubidium cell is simply inserted in a copper ring on which two high power resistors ( $67\ \Omega$ , 10 mW maximal power) are glued and used to heat the sample (see figure 5(b)). All contacts are realized with heat pasting grease and the ensemble is finally isolated using aluminium paper. An optical window is cut inside the copper ring in order to collect the blue fluorescence, using an imaging lens, an interferometric filter centred at the wavelength  $\lambda = 420\text{ nm}$ , used to isolate the fluorescence from scattered light, and a photomultiplier.

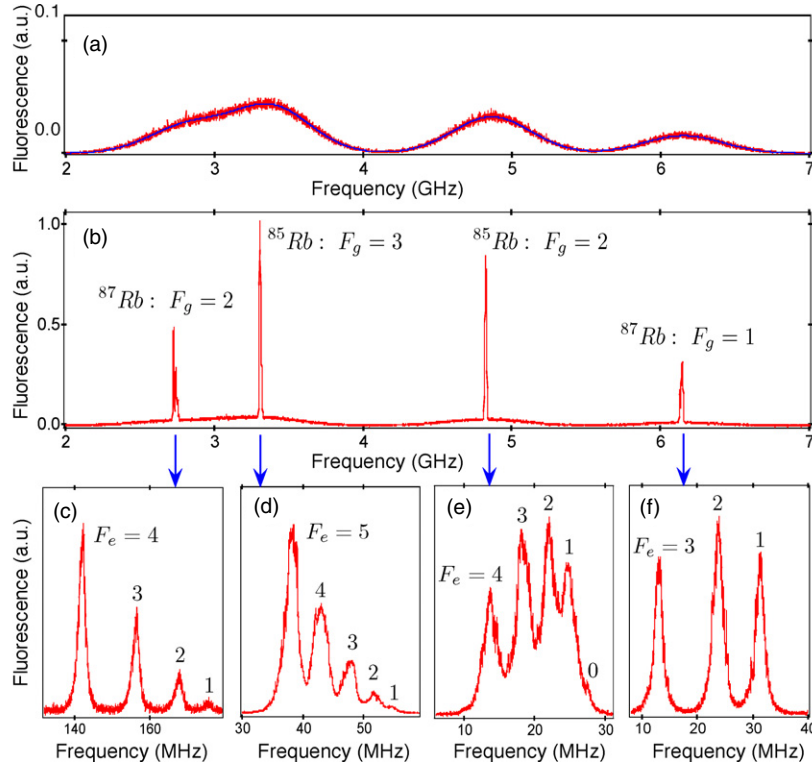


**Figure 6.** (a) Fluorescence spectrum of the  $5S_{1/2} \rightarrow 5D_{5/2}$  two-photon transition in rubidium, when the retroreflected beam is misaligned. Blue solid line corresponds to a fit of the data with four Gaussian functions, which correspond to the ground-state hyperfine levels of  $^{85}\text{Rb}$  and  $^{87}\text{Rb}$ . Energy differences in terms of laser frequency are related to hyperfine energy splittings by a factor one half. (b) Doppler-free spectrum of the  $5S_{1/2} \rightarrow 5D_{5/2}$  two-photon transition in rubidium. (c)–(f) Hyperfine structure of the excited state  $5D_{5/2}$  for  $^{85}\text{Rb}$  and  $^{87}\text{Rb}$ .  $F_g$  and  $F_e$  are respectively related to the total angular momentum of the hyperfine levels on the ground state and on the excited state. Data fitting with Lorentzian functions leads to  $\delta[(1 \leftrightarrow 2)]_{^{87}\text{Rb}} = 15 \pm 1$  MHz,  $\delta[(2 \leftrightarrow 3)]_{^{87}\text{Rb}} = 22 \pm 1$  MHz,  $\delta[(3 \leftrightarrow 4)]_{^{87}\text{Rb}} = 28 \pm 1$  MHz,  $\delta[(1 \leftrightarrow 2)]_{^{85}\text{Rb}} = 5 \pm 1$  MHz,  $\delta[(2 \leftrightarrow 3)]_{^{85}\text{Rb}} = 8 \pm 1$  MHz,  $\delta[(3 \leftrightarrow 4)]_{^{85}\text{Rb}} = 10 \pm 1$  MHz, and  $\delta[(4 \leftrightarrow 5)]_{^{85}\text{Rb}} = 9 \pm 1$  MHz, where  $\delta[(i \leftrightarrow j)]$  is the energy splitting between hyperfine sublevels  $F_e = i$  and  $F_e = j$ .

### 5.3. Results

Two-photon absorption spectra are recorded by scanning the frequency of the laser diode and detecting the fluorescence from the  $5D_{5/2} \rightarrow 6P_{3/2} \rightarrow 5S_{1/2}$  radiative cascade decay. When the retroreflected beam is misaligned, Doppler-broadened absorption spectra, which arise from the absorption of two photons from the same laser beam, are measured. As depicted in figure 6(a), four lines corresponding to the hyperfine ground states of  $^{85}\text{Rb}$  and  $^{87}\text{Rb}$  are observed. However it is not possible to resolve excited state hyperfine structure, which remains hidden by Doppler broadening. By fitting each line with a Gaussian profile and using relation (5), the temperature of the atomic vapour in the interaction volume can be estimated. A temperature of about 140 °C is achieved, which corresponds to optimal detection of the two-photon absorption process, as discussed in the previous section.

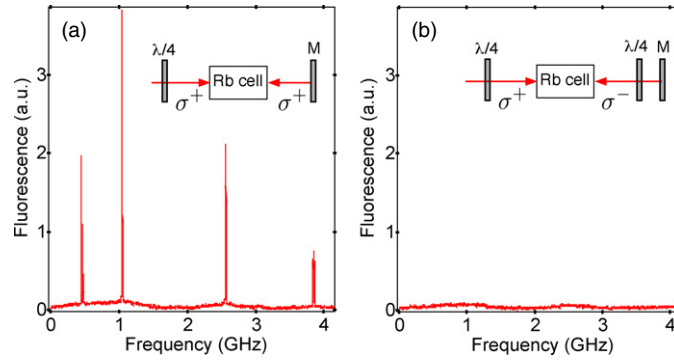


**Figure 7.** Illustration of two-photon transition selection rule  $\Delta m_F = 2$ , by changing the beam polarizations. (a) Fluorescence spectrum with two counterpropagating beams with identical polarization  $\sigma^+$  and (b) with opposite circular polarizations  $\sigma^+$  and  $\sigma^-$ .

When the retroreflected beam is properly aligned, Doppler-free two-photon absorption spectrum is evidenced as depicted in figure 6(b). Strong fluorescence peaks at atomic resonant frequencies are superimposed on the remaining weak Doppler broadened profile. As a two-photon transition is considered, energy difference in terms of laser frequency is related to energy splitting of the atom by a factor one half. The ground-state hyperfine splitting is then measured to be  $3.03 \pm 0.03$  GHz for  $^{85}\text{Rb}$  and  $6.83 \pm 0.06$  GHz for  $^{87}\text{Rb}$ , in excellent agreement with other published values [28].

The hyperfine structure of the excited state  $5D_{5/2}$  is then studied by reducing the frequency scanning range of the laser diode and zooming on the resonances of the two-photon absorption profile. As depicted in figures 6(c)–(f), all the hyperfine levels of the  $5D_{5/2}$  excited state are properly resolved, except  $F_e = 0$  for  $^{85}\text{Rb}$ . Even if the precision of the measurements is poor, due to laser diode instabilities, the measured spectral features are again in agreement with precise measurements given in [28]. Note that such an experiment also illustrates the selection rule on the total angular momentum  $\Delta F = 0, \pm 1, \pm 2$  for the two-photon absorption process [22, 25, 29].

For the data depicted in figure 6, the linewidths of the resonant peaks, measured in terms of laser frequency, are on the order of 2 MHz, which is close to the spectral bandwidth of the laser diode. The lifetime of the  $5D_{5/2}$  excited state is about 266 ns, leading to a natural width of the transition around  $2\gamma = 600$  kHz [28]. As two-photon transitions are considered, the measured width in terms of laser frequency is related to the transition linewidth by a factor one-half. To evidence the natural width of the transition, a laser with less than 300 kHz spectral bandwidth would then be required.

The experiment can be used to illustrate two-photon absorption selection rules associated with the total angular momentum projection  $m_F$ , by changing the laser beam polarizations [29]. As mentioned before, the introduction of a quarter wave plate before the rubidium cell allows one to excite the atoms with two counterpropagating beams with identical circular polarizations  $\sigma^+$ . In that condition, the two-photon transition selection rule  $\Delta m_F = 2$  is always fulfilled by absorbing two photons, and a strong Doppler-free signal is observed. Besides, if a second quarter-wave plate is introduced in front of the reflecting mirror, the polarization of the retroreflected beam becomes  $\sigma^-$ . The absorption of two photons from opposite directions would then lead to  $\Delta m_F = 0$  which is forbidden owing to the selection rule for a two-photon transition such that  $\Delta l = 2$  [29]. In that case, no Doppler-free signal is observed, as depicted

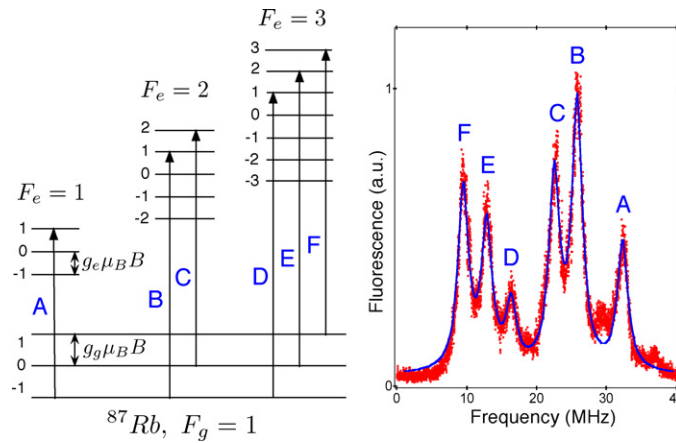


**Figure 8.** Zeeman splitting of the transitions between  $5S_{1/2}$ ,  $F_g = 1$  and  $5D_{5/2}$  of  $^{87}\text{Rb}$ , when a magnetic field  $B$  is applied to the rubidium cell. A, B, C, D, E, F are related to the six transitions fulfilling the selection rule  $\Delta m_F = 2$ . The magnetic field is applied along the direction of laser propagation.

in figure 7. However, the Doppler-broadened profile is still present because it corresponds to the absorption of two photons from the same beam ( $\Delta m_F = 2$ ). Note that the experimental configuration using two quarter-wave plates would be the optimal situation for the investigation of  $S \rightarrow S$  transition ( $\Delta l = 0$ ), like the  $5S_{1/2} \rightarrow 7S_{1/2}$  transition in rubidium. In that case, the profile of the absorption spectra is just a Lorentzian curve, as the absorption of two photons from the same beam is forbidden ( $\Delta m_F = 2$ ). The Doppler-broadened profile can then be eliminated for that particular case [25, 27].

As a final experiment, a permanent magnet is put close to the cell in order to observe Zeeman splitting. A typical result is depicted in figure 8 for the transition  $5S_{1/2}$ ,  $F_g = 1 \leftrightarrow 5D_{5/2}$  of  $^{87}\text{Rb}$ . The transition through  $F_e = 1$  is not split, the one through  $F_e = 2$  is split into two lines and the one through  $F_e = 3$  is split into three lines. Such a result is another experimental illustration of the transition selection rule  $\Delta m_F = 2$  (see figure 8).

In terms of energy, the splitting between consecutive Zeeman levels in the ground state is equal to  $g_g \mu_B B$ , where  $g_g$  is the electron gyromagnetic factor in the ground state,  $\mu_B$  is the Bohr magneton and  $B$  is the magnetic field magnitude (see figure 8). For the excited state, the Zeeman level splitting follows the same relation replacing  $g_g$  by the electron gyromagnetic factor in the excited state  $g_e$ . As a result, it is straightforward to show that the frequency splitting of transitions associated with a given value of the excited state total angular momentum  $F_e$  is given by  $(g_e - g_g) \mu_B B$ .

A systematic study of Zeeman splitting as a function of the magnetic field magnitude has not been performed yet. As a next step, we plan to introduce the rubidium cell inside coils in order to have better control of the magnitude and the orientation of the applied magnetic field. This configuration would allow one to measure the parameter  $(g_e - g_g)$  or to use the Doppler-free two-photon absorption spectrum as an atomic magnetometer.

## 6. Conclusion

While atomic physics may be considered by students as a theoretical subject, we present here experiments enabling advanced undergraduates to become acquainted with spectroscopy

techniques widely used in laboratories. Throughout this paper, we have implemented two complementary methods of high-resolution spectroscopy—saturated absorption and two-photon spectroscopy—to probe the hyperfine structure of rubidium. Eventually, these experiments combined within a single setup, constitute a great opportunity for students to investigate atomic spectra and to illustrate quantum mechanics selection rules as well as Zeeman effect.

## Acknowledgments

The authors are grateful to F Biraben for fruitful discussions and C Ollier for technical support. We acknowledge financial support by Ecole Normale Supérieure de Cachan.

## References

- [1] Ricci L, Weidemüller M, Esslinger T, Hemmerich A, Zimmermann C, Vuletic V, König W and Hänsch T W 1995 A compact grating-stabilized diode laser system for atomic physics *Opt. Commun.* **117** 541–9
- [2] Arnold A S, Wilson J S and Boshier M G 1998 A simple extended-cavity diode laser *Rev. Sci. Instrum.* **69** 1236–9
- [3] MacAdam K B, Steinbach A and Wieman C 1992 A narrow-band tunable diode laser system with grating feedback, and a saturated absorption spectrometer for Cs and Rb *Am. J. Phys.* **60** 1098–111
- [4] Preston D W 1996 Doppler-free saturated absorption: laser spectroscopy *Am. J. Phys.* **64** 1432–6
- [5] Libbrecht K G and Libbrecht M W 2006 Interferometric measurement of the resonant absorption and refractive index in rubidium gas *Am. J. Phys.* **74** 1055–60
- [6] Leahy C, Hastings J T and Wilt P M 1996 Temperature dependence of Doppler-broadening in rubidium: an undergraduate experiment *Am. J. Phys.* **65** 367–71
- [7] Van Baak D A 1996 Resonant Faraday rotation as a probe of atomic dispersion *Am. J. Phys.* **64** 724–35
- [8] Olson A J, Carlson E J and Mayer S K 2006 Two-photon spectroscopy of rubidium using a grating-feedback diode laser *Am. J. Phys.* **74** 218–23
- [9] The grating-feedback laser diode system can be built by undergraduates as described in Conroy R S, Carleton A, Carruthers A, Sinclair B D, Rae C F and Dholakia K 2000 A visible extended cavity diode laser for the undergraduate laboratory *Am. J. Phys.* **68** 925–31
- [10] The description of a low cost Michelson wavelength-meter is provided in Fox P J, Scholten R E, Walkiewicz M R and Drullinger R E 1999 A reliable, compact, and low-cost Michelson wavemeter for laser wavelength measurement *Am. J. Phys.* **67** 624–30
- [11] Smith P W and Hänsch T W 1971 Cross-relaxation effects in the saturation of the 6328-Å neon-laser line *Phys. Rev. Lett.* **26** 740–3
- [12] Hänsch T W, Shahin I S and Schawlow A L 1971 High-resolution saturation spectroscopy of the sodium D lines with a pulsed tunable dye laser *Phys. Rev. Lett.* **27** 707–10
- [13] Bordé C 1970 Spectroscopie d'absorption saturée de diverses molécules au moyen des lasers à gaz carbonique et à protoxyde d'azote *C. R. Acad. Sci. Paris* **271B** 371
- [14] Schalow A L 1981 Nobel Lecture reproduced in *Rev. Mod. Phys.* **54** 697–707
- [15] Grynberg G, Aspect A and Fabre A 1997 *Introduction aux Lasers et l'Optique quantique* (Paris: Ellipses)
- [15] Grynberg G, Aspect A and Fabre A 2009 *An Introduction to Laser Physics and Quantum Optics* (Cambridge: Cambridge University Press) (The English version)
- [16] Cahuzac P, Robaux O and Vetter R 1976 Pressure-broadening studies of the 3.51  $\mu\text{m}$  line of xenon by saturated-amplification techniques *J. Phys. B: At. Mol. Phys.* **9** 3165–72
- [17] Cagnac B, Plimmer M D, Julien L and Biraben F 1994 The hydrogen atom, a tool for metrology *Rep. Prog. Phys.* **57** 853–93
- [18] Hall J L, Bordé C and Uehara K 1976 Direct optical resolution of the recoil effect using saturated absorption spectroscopy *Phys. Rev. Lett.* **37** 1339–42
- [19] Letokhov V S 1977 *Nonlinear Laser Spectroscopy* (New York: Springer)
- [20] Vasilenko L S, Chebotaev V P and Shishaev A V 1970 Line shape of two-photon absorption in a standing-wave field in a gas *JETP Lett.* **12** 161–5
- [21] Biraben F, Cagnac B and Grynberg G 1974 Experimental evidence of two-photon transition without Doppler broadening *Phys. Rev. Lett.* **32** 643–5
- [22] Grynberg G 1976 *Thèse d'état* Université Paris 6; available online at <http://tel.archives-ouvertes.fr/docs/00/06/09/65/PDF/1976GRYNBERG.pdf>
- [23] Levenson M D and Bloembergen N 1974 Observation of two-photon absorption without Doppler-broadening on the 3S–5S transition in sodium vapor *Phys. Rev. Lett.* **32** 645–8

- [24] Schwob C, Jozefowski L, de Beauvoir B, Hilico L, Nez F, Julien L, Biraben F, Aef O and Clairon A 1999 Optical frequency measurement of the 2S–12D transitions in hydrogen and deuterium: Rydberg constant and Lamb shift determinations *Phys. Rev. Lett.* **82** 4960–3
- [25] Grynberg G and Cagnac B 1977 Doppler-free multiphotonic spectroscopy *Rep. Prog. Phys.* **40** 791–841
- [26] Ryan R E, Westling L A and Metcalf H J 1993 Two-photon spectroscopy in rubidium with a diode laser *J. Opt. Soc. Am. B* **10** 1643–8
- [27] Ko M S and Liu Y W 2004 Observation of rubidium  $5S_{1/2} \rightarrow 7S_{1/2}$  two-photon transitions with a diode laser *Opt. Lett.* **29** 1799–801
- [28] Nez F, Biraben F, Felder R and Millerioux Y 1993 Optical frequency determination of the hyperfine components of the  $5S_{1/2}$ – $5D_{3/2}$  two-photon transitions in rubidium *Opt. Commun.* **102** 432
- [29] Cagnac B, Grynberg G and Biraben F 1973 Spectroscopie d'absorption multiphotonique sans effect Doppler *J. Physique* **34** 845–58